Charge-transfer satellites in the 2p core-level photoelectron spectra of heavy-transition-metal dihalides

Jaehoon Park, Seungoh Ryu, Moon-sup Han, and S.-J. Oh*
Department of Physics, Seoul National University, Seoul 151, Korea
(Received 21 October 1987; revised manuscript received 8 February 1988)

We extend the charge-transfer model with the core-hole–3*d*-electron Coulomb attraction [van der Laan *et al.*, Phys. Rev. B **23**, 4369 (1981)] to the 2*p* core-level photoemission satellite structures of cobalt, iron, and manganese dihalides. This model was found to account for the positions and intensities of satellites and main peaks very well with reasonable values of parameters. These parameter values show the expected trends not only along the ligand series from fluorine to bromine but also along the transition-metal series from copper to manganese. This gives us confidence that the charge-transfer mechanism is responsible for the satellite structures in the 2*p* core-level photoemission spectra of heavy-transition-metal compounds, and that the screening response is important even for insulators in the presence of a core hole. It also suggests the core-level photoemission spectra, if properly understood, can be used to obtain parameters on the valence-electronic structures.

I. INTRODUCTION

Satellite structures in core-level x-ray photoemission spectroscopy (XPS) data have been studied by many authors and their origins have been the source of active debate for a long time.[1–7] These various satellites, sometimes called "shakeup" or "shakedown" satellites depending on whether they lie in the higher- or lower-binding-energy sides of the most intense "main line," are usually more prominent in rare-earth-metal ($4f,5f$) and transition-metal ($3d,4d$) compounds where electron correlation effects are strong. Recently, for the case of metallic $4f$ lanthanide compounds, considerable progress has been made by combined efforts of theorists and experimentalists in understanding the origin of these satellite structures.[8–12] Basically, core-level XPS spectrum can be well described by the Anderson-impurity-type Hamiltonian, and the Coulomb attraction between the core hole and localized valence electrons and the resulting screening response have to be taken into account. This success has been recently extended to insulating $4f$ compounds as well,[13] and these satellites, if properly interpreted, turned out to be the source of a wealth of information on the valence-level electronic structure of these compounds. By analyzing the energy separations and the intensity distributions between $3d$ core-level satellites and main peaks, we can obtain information on the $4f$-level energy positions, Coulomb correlation energies, and the hybridization strength between the $4f$ and the conduction-electron states.[9,10,12,13]

In the case of $3d$ transition-metal compounds, the situation is not so clear. There are still several competing models for the origin of the core-level satellites, none of which seems to be universally accepted. At least five different models have been proposed for the occurrence of satellites in the $2p$ core-level XPS of $3d$ transition-metal compounds. One model attributes the satellite structure to the multiplet and crystal-field splittings of the $2p^5 3d^n$ unfilled-shell configurations. Although calculations actually predict significant energy spreads of multiplet structures in the $2p^5 3d^n$ configuration,[14] the fact that $1s$ core-level XPS also shows satellite structures similar to the $2p$ spectrum[5] suggests that this mechanism is unlikely to be the origin of the satellites. Other models propose that the shakeup of one valence electron accompanying the photoionization process generates the satellite structure—the shakeup mechanism could either be of intra-atomic type[15] from the metal $3d$ state to the unoccupied metal $4sp$ state, or of charge-transfer type[16] from the ligand state to the metal $3d$ state. There have been various arguments for and against these models,[1] but neither of these models is entirely satisfactory. For example, the metal $3d$-to-$4sp$ shakeup model cannot explain the absence of satellites in Cu^+ compounds (d^{10} configuration), whereas the ligand-to-metal charge-transfer model cannot explain the fact that some Cu^{2+} compounds (d^9 configuration) have two satellite peaks, since the satellite in this case should have d^{10} configuration which does not have any multiplet splitting.

Most of the above models do not explicitly take into account the screening or relaxation process in the final state of XPS where a core hole is created. However, for metallic systems it is now realized that strong Coulomb attraction between the core hole and the localized $3d$ or $4f$ levels makes the neutral "excitonic" state, where the core hole is neutralized by an extra screening electron in the $3d$ or $4f$ level, the lowest-energy state in the presence of a core hole.[17,18] This screening argument is generally given only for metallic systems, but Larsson[19] calculated that even for insulating $3d$ transition-metal compounds such as Cu^{2+} dihalides (d^9 configuration), the lowest-energy state in the presence of a core hole corresponds to the fully screened state with approximately an extra $3d$ electron for screening. Therefore, he proposed that the main peak in the $2p$ XPS spectrum corresponds to the d^{10} configuration, whereas satellites correspond to the d^9 configuration. This is in marked contrast to earlier shakeup satellite models[15,16] where the final state corre-

sponding to the main peak is assumed to have the same valence-electronic configurations as the initial ground state. Later, Veal and Paulikas[20] confirmed from their atomic calculations on many $3d$ transition-metal elements that the lowest-energy state in the presence of a core hole corresponds to the state where screening is done by the local $3d$ electrons. They, however, proposed that the satellites arise from the final states where the nonlocal $2s$ or $4p$ state of metal screens the core hole in contrast to the Larsson model. But the shortcoming of this model is that they were concerned only with the energy separation between the main and satellite peaks but did not consider the intensity ratio between them.

Several years ago, van der Laan *et al.*[21] suggested the charge-transfer model for copper dihalides which is consistent with the interpretation of Larsson[19] and described the physics in terms of a few parameters. They used the Anderson-impurity-type model Hamiltonian similar to the metallic cases[8-10] to describe the $2p$ core-level XPS spectra of insulating copper dihalides, where d-d Coulomb repulsion energy U, the charge-transfer energy Δ, the ligand p–metal d hybridization energy T, and the core-hole–d-electron Coulomb attraction energy Q are taken into account. They were able to fit both intensities and energy positions of the $2p$ core-level satellites using this model Hamiltonian with reasonable parameter values. Later this model was successfully applied to the $2p$ satellite structures of nickel dihalides.[22,23] From the results of the fit, they were able to obtain useful information on the valence-electronic structures of these compounds, such as d-d Coulomb energy, ligand $2p$–metal $3d$ energy difference, and their mixing strength. Hence, if this charge-transfer model is correct, the core-level XPS satellites can be used to study valence-electronic structures indirectly, as in the case of $4f$ rare-earth-metal compounds.[9-13] In this paper, we will extend this charge-transfer model to other heavy $3d$ transition-metal dihalides (cobalt, iron, and manganese dihalides) to see whether this model can explain satellite structures of these insulating compounds as well.

II. MATERIALS AND DATA

The materials we have studied were cobalt dihalides (CoF_2, $CoCl_2$, and $CoBr_2$), iron dihalides (FeF_2, $FeCl_2$, and $FeBr_2$), and manganese dihalides (MnF_2, $MnCl_2$, and $MnBr_2$). The transition-metal cations in these dihalides are located in a distorted octahedron formed by the nearest-neighbor anions. The distortions are either rhombohedral or tetragonal type, but since they are small we can neglect them for our purposes here. Subsequently we will consider the compounds as having a cubic symmetry around the cations.

The $3d$ level in a octahedral surrounding is split into e_g (doublet) and t_{2g} (triplet) levels by the crystal field, and the energy difference between the two levels is denoted by $10Dq$ determined by the strength of the crystal potential. The ground states of the cations (d^7, d^6, and d^5 configurations for Co^{2+}, Fe^{2+}, and Mn^{2+}, respectively) in the cubic crystal are determined by the competition between this splitting energy $10Dq$ and electrostatic Coulomb energy.[24] For the systems we studied here, the Coulomb energy is dominant and the ground state are all high spin states.[24-26] Therefore, for Co^{2+} ions with d^7 configuration, the ground state has the ${}^4T_{1g}\ (t_{2g})^5(e_g)^2$ configuration, and for Fe^{2+} (d^6) and Mn^{2+} (d^5) ions, the ground states are ${}^5T_{2g}\ (t_{2g})^4(e_g)^2$ and ${}^6A_{1g}\ (t_{2g})^3(e_g)^2$, respectively.

We will discuss only $2p_{3/2}$ core-level XPS spectra of these compounds. The $2p_{1/2}$ spectra were sometimes found to be considerably different from the $2p_{3/2}$ spectra because of the influence from strong interference between valence-electron rearrangement and the near-threshold Coster-Kronig decay,[27] and hence are not considered here. The experimental data were taken from published literature. The fluoride compound data (CoF_2, FeF_2, and MnF_2) were taken from Ref. 7, and all others from Ref. 28. From these raw spectra we made appropriate x-ray satellite corrections and inelastic electron background corrections. The method used for the background correction is a simple way[29] in which the ratio of electrons ejected via inelastic scatterings to those with no scattering is regarded as constant independent of the amount of the energy loss. We tried to fit the resulting corrected $2p_{3/2}$ spectra with the theoretical model calculations discussed in the next section.

III. CHARGE-TRANSFER MODEL CALCULATIONS

We now extend the charge-transfer model of Larsson[19] and Sawatzky *et al.*[21-23] to cobalt, iron, and manganese dihalide cases. We will in this section use the cluster approximation where the band nature of the ligand $2p$ states is neglected. The effect of the ligand-level energy dispersion will be briefly discussed later in Sec. V. Since this model has been described in detail and applied to nickel compounds[23] before, we will only mention essential points of the model and extensions necessary for a larger number of d holes here.

The ground state of the system is considered to be a mixture of the purely ionic configuration $|d^n\rangle$ ($n=5,6,7$ here) and the charge-transfer states $|d^{n+1}\underline{L}\rangle$, $|d^{n+2}\underline{L}^2\rangle, \ldots, |d^{10}\underline{L}^{10-n}\rangle$, where one or more electrons are transferred to the $3d$ level from neighboring ligand $2p$ orbitals. ($\underline{L}$ denotes the hole in the ligand $2p$ level.) For this mixing to occur, the charge-transfer states should have the same symmetry as the $|d^n\rangle$ state. If we assume that the mixing matrix elements between the ligand and the transition-metal $3d$ levels are the same for both e_g- and t_{2g}- symmetry state and also neglect the energy difference $10Dq$ for simplicity of calculation (it turns out that for the parameter ranges we will get, this is not a bad approximation—see Sec. V), then the states we have to consider are

$$|d^n\rangle = |\underline{d}_\alpha \underline{d}_\beta \underline{d}_\gamma \cdots\rangle ,$$

$$|d^{n+1}\underline{L}\rangle = \frac{1}{\sqrt{10-n}}\left(|\underline{L}_\alpha \underline{d}_\beta \underline{d}_\gamma \cdots\rangle + |\underline{d}_\alpha \underline{L}_\beta \underline{d}_\gamma \cdots\rangle + \cdots\right),$$

$$|d^{n+1}\underline{L}^2\rangle=\left[\frac{2}{(10-n)(9-n)}\right]^{1/2}\times(|\underline{L}_\alpha\underline{L}_\beta\underline{d}_\gamma\cdots\rangle+|\underline{d}_\alpha\underline{L}_\beta\underline{L}_\gamma\cdots\rangle+\cdots),$$

$$\cdots,$$

$$|d^{10}\underline{L}^{10-n}\rangle=|\underline{L}_\alpha\underline{L}_\beta\underline{L}_\gamma\cdots\rangle,$$

where $\underline{d}_\alpha,\underline{d}_\beta$ denote holes in the e_g orbital, and $\underline{d}_\gamma,\underline{d}_\delta,\underline{d}_\epsilon$ denote holes in the t_{2g} orbital. The diagonal Hamiltonian matrix elements from these states are

$$\langle d^n|H|d^n\rangle=0,\ \text{reference},$$
$$\langle d^{n+1}\underline{L}|H|d^{n+1}\underline{L}\rangle=\Delta,$$
$$\langle d^{n+2}\underline{L}^2|H|d^{n+2}\underline{L}^2\rangle=2\Delta+U,$$
$$\langle d^{n+3}\underline{L}^3|H|d^{n+3}\underline{L}^3\rangle=3\Delta+3U,$$
$$\cdots.$$

where Δ is the energy required to transfer one electron from the ligand $2p$ to the metal $3d$ states,

$$\Delta=E(d^{n+1}\underline{L})-E(d^n),$$

and U is the effective Coulomb interaction between $3d$ electrons.

If we define the one-electron mixing matrix element T between the ligand and metal $3d$ levels,

$$T=\langle\underline{d}_\alpha|H|\underline{L}_\alpha\rangle=\langle\underline{d}_\beta|H|\underline{L}_\beta\rangle=\langle\underline{d}_\gamma|H|\underline{L}_\gamma\rangle=\cdots,$$

(assumed to be the same for both e_g and t_{2g} orbitals) then the off-diagonal elements of the Hamiltonian are

$$\langle d^n|H|d^{n+1}\underline{L}\rangle=\sqrt{(10-n)}T,$$
$$\langle d^{n+1}\underline{L}|H|d^{n+2}\underline{L}^2\rangle=\sqrt{2(9-n)}T,$$
$$\langle d^{n+2}\underline{L}^2|H|\underline{d}^{n+3}\underline{L}^3\rangle=\sqrt{3(8-n)}T,$$
$$\cdots,$$
$$\langle d^9\underline{L}^{9-n}|H|d^{10}\underline{L}^{10-n}\rangle=\sqrt{(10-n)}T,$$

and all other off-diagonal elements are zero. The wave function of the initial ground state can be determined by diagonalizing the above Hamiltonian matrix and can be written as

$$|\Psi_G\rangle=a|d^n\rangle+b|d^{n+1}\underline{L}\rangle+c|d^{n+2}\underline{L}^2\rangle+\cdots+f|d^{10}\underline{L}^{10-n}\rangle,$$

with

$$|a|^2+|b|^2+\cdots+|f|^2=1.$$

For Co^{2+}, Fe^{2+}, and Mn^{2+} compounds, we have to diagonalize 4×4, 5×5, and 6×6 Hamiltonian matrices, respectively.

The eigenfunctions in the XPS final state with a core hole can be calculated in a similar way, but since the core hole created in the photoionization pulls down the $3d$ energy levels due to the Coulomb attraction, the diagonal Hamiltonian matrix elements will change. We can take the following states as the basis:

$$|\underline{c}d^n\rangle,|\underline{c}d^{n+1}\underline{L}\rangle,|\underline{c}d^{n+2}\underline{L}^2\rangle,\ldots,|\underline{c}d^{10}\underline{L}^{10-n}\rangle,$$

where $\underline{c}$ denotes a core hole, and then the diagonal elements are

$$\langle\underline{c}d^n|H|\underline{c}d^n\rangle=E_c,$$
$$\langle\underline{c}d^{n+1}\underline{L}|H|\underline{c}d^{n+1}\underline{L}\rangle=E_c+\Delta-Q,$$
$$\langle\underline{c}d^{n+2}\underline{L}^2|H|\underline{c}d^{n+2}\underline{L}^2\rangle=E_c+2(\Delta-Q)+U,$$
$$\langle\underline{c}d^{n+2}\underline{L}^3|H|\underline{c}d^{n+3}\underline{L}^3\rangle=E_c+3(\Delta-Q)+3U,$$
$$\cdots.$$

Here E_c is the core-hole energy relative to the ionic lat-

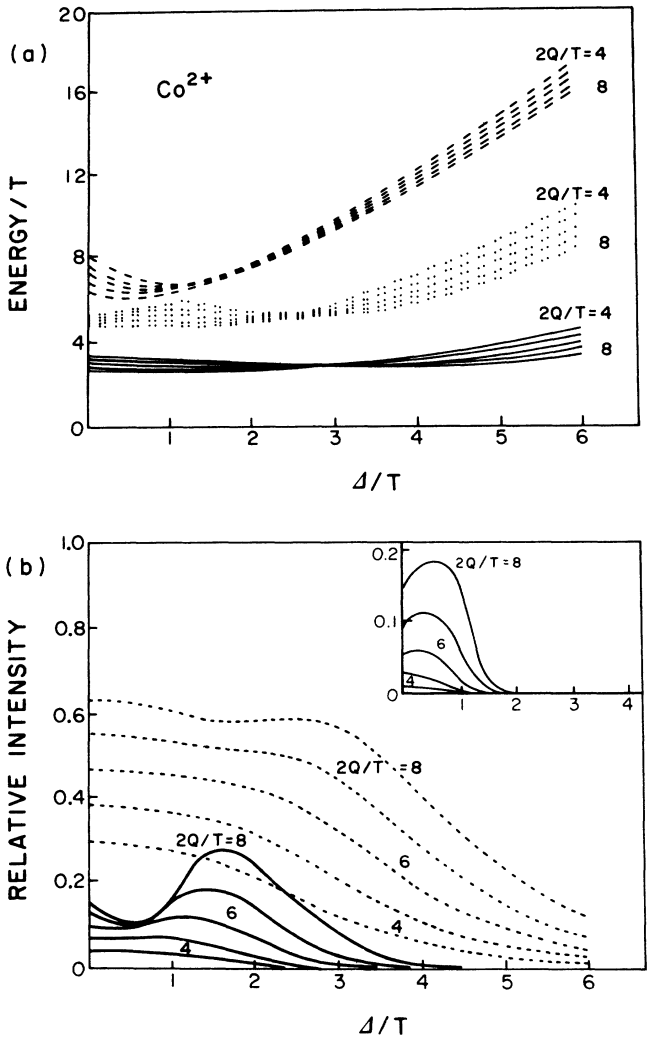

FIG. 1. Theoretical curves for cobalt compounds from the cluster model calculation as a function of Δ/T for $2Q/T=4$, 5, 6, 7, and 8. (a) Energy differences of satellites relative to the main peak in units of T. (b) Relative intensities of satellites to the main peak. The dashed line is for the first satellite, the solid line is for the second satellite, and the line in the inset is for the third satellite.

tice, and Q is the effective core-hole–$3d$-electron Coulomb attraction. Q, as defined above, is positive and lowers the energy of the charge-transferred states relative to the $|d^n\rangle$ state. We assume that off-diagonal elements remain the same as in the initial state, i.e., the change in the hybridization energy produced by the core hole is neglected.

Now with eigenfunctions of the initial ground state and the final states with a core hole obtained as above, we can get the XPS spectrum using the sudden approximation for photoionization cross section:

$$\rho(\varepsilon_k) \propto \sum_{i=1}^{10-n+1} |\langle \Psi_i | \underline{c}\Psi_G \rangle|^2 \delta(\hbar\omega - \varepsilon_k - E_i) .$$

Here $\hbar\omega$ is the photon energy, ε_k the kinetic energy of the photoelectron, and E_i the final-state eigenenergies of the $(N-1)$-electron system with a core hole. $|\underline{c}\Psi_G\rangle$ represents the state obtained by annihilating a core electron in the ground state keeping other orbitals "frozen." This equation gives positions and intensities of possible core-level XPS peaks. Depending on the parameter values of Δ, T, U, and Q, the energy separations and intensity ratios of various peaks will change.

To facilitate a search for best parameter values that fit the experimental spectra, we make plots of line positions and intensities as a function of Δ, T, U, and Q for each case of d^7 (Co^{2+}), d^6 (Fe^{2+}), and d^5 (Mn^{2+}) configurations. These are shown in Figs. 1, 2, and 3. In Fig. 1(a), we plot the energy separations of the first, second, and third satellites from the main peak (lowest-

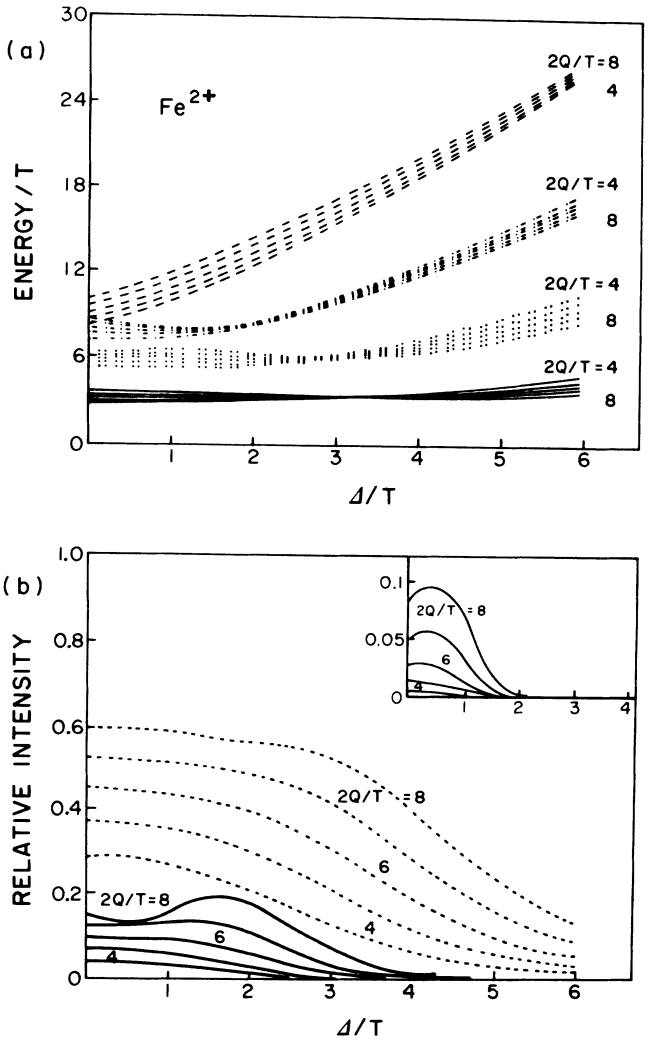

FIG. 2. Theoretical curves for iron compounds from the cluster model calculation as a function of Δ/T for $2Q/T=4$, 5, 6, 7, and 8. (a) Energy differences of satellites relative to the main peak in units of T. (b) Relative intensities of satellites to the main peak. The dashed line is for the first satellite, the solid line is for the second satellite, and the line in the inset is for the third satellite.

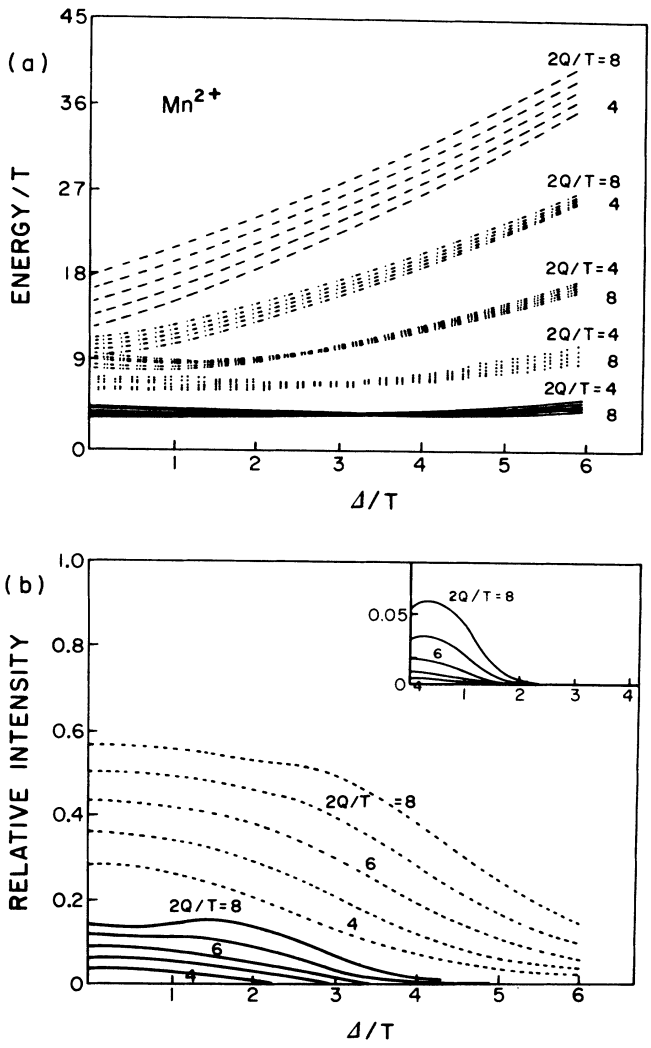

FIG. 3. Theoretical curves for manganese compounds from the cluster model calculation as a function of Δ/T for $2Q/T=4$, 5, 6, 7, and 8. (a) Energy differences of satellites relative to the main peak in units of T. (b) Relative intensities of satellites to the main peak. The dashed line is for the first satellite, the solid line is for the second satellite, and the line in the inset is for the third satellite.

binding-energy peak) for cobalt dihalides. (There are four final-state eigenstates.) The intensities of these satellites relative to the main peak are plotted in Fig. 1(b). In both figures, all energies are in units of T and we assumed $U/Q=0.7$ as in previous calculations.[22,23] We took the parameter range representative for cobalt dihalides CoF_2, $CoCl_2$, and $CoBr_2$. Similar figures for iron and manganese compounds are shown in Figs. 2 and 3. There are four satellites for iron dihalides and five for manganese dihalides, but intensities of these other than the first three are negligibly small. Therefore, in Figs. 2(b) and 3(b), we plot only the intensities of the first, second, and third satellites relative to the main peak.

IV. RESULTS OF THE FIT AND ANALYSIS

We first decompose the experimental $2p_{3/2}$ spectra into a sum of two or three Lorentzians. [For cobalt compounds, Fig. 1(b) shows the third satellite can have an appreciable intensity in some parameter range, but it turns out that for all three cobalt compounds we consider here, the parameter values are outside this range.] We list the resulting binding-energy differences and intensities of satellite peaks relative to the main peak for each compound in Table I. Here the intensity ratio is obtained by the area under the peak. We then try to obtain these energy separations and intensity ratios by varying parameter values of Δ, T, U, and Q. But here we impose an important restriction—we keep the values of T, U, and Q fixed for a given cation (transition-metal ion) and vary only Δ depending on the ligand. The reason is that we expect the d-d Coulomb interaction energy U and the core-hole–d-electron Coulomb attraction energy Q to be essentially independent of ligands because these are mostly determined by atomic parameters. The hybridization T between metal d level and ligand p level may well vary depending on the ligand, but it is also found to be essentially constant[23,30] because of the canceling effect between the lattice parameter and the ligand wave-function radial extent. On the other hand, the charge-transfer energy will depend strongly on the ligand because of different ligand electronegativity values. Hence, we assumed the values of three parameters T, U, and Q the same for a given transition-metal element, but changed Δ to fit the experimental satellite positions and intensities for all three ligands. It is by no means *a priori* clear that this procedure is possible. The fact that it is possible and we get parameter values which are reasonable and show the expected chemical trends gives us the confidence that we understood the basic physics on the origin of $2p$ core-level satellite structure.

We will illustrate how these parameter values are determined by showing an example of a cobalt dihalide case. The relative intensities of the first and second satellites in $CoCl_2$ are 48% and 10%, respectively, from Table I. This puts $Q/T\approx 3.5$ and $\Delta/T\approx 2.5$ from the theoretical intensity curves of Fig. 1(b). Since the energy separation of the first satellite from the main peak with these parameter values is given by $\Delta E/T\approx 3.1$ from Fig. 1(a), this gives T a value of 1.8 eV by comparing with the experimental value of ΔE. This also gives about the correct second-satellite energy separation. Now for CoF_2 and $CoBr_2$, we follow the curve with $Q/T\approx 3.5$ and change only Δ/T in Fig. 1 to get the satellite intensities and energy separations consistent with the experimental values in Table I. This procedure gives $\Delta/T\approx 4.5$ for CoF_2 and $\Delta/T\approx 1.5$ for $CoBr_2$. We follow similar procedures for iron and manganese dihalides as well.

We show the best fits for cobalt, iron, and manganese dihalides from this procedure in Figs. 4, 5, and 6, respectively, combining the experimental spectra (dots) and the theoretical curves (solid lines). We included the Gaussian broadening of 1.2 eV full width at half maximum (FWHM) for instrumental resolution, and various amounts of Lorentzian broadening to mimic lifetime and multiplet effects. We see that the agreement between theory and experiment is very good for all the compounds, considering many restrictions on the fit procedure.

In Table II we list values of the parameters Δ, U, T, and Q for these best-fit results. We also included the ground-state $3d$ electron occupation number $\langle n_d \rangle$ in the last column. To see the trends as we change cations more

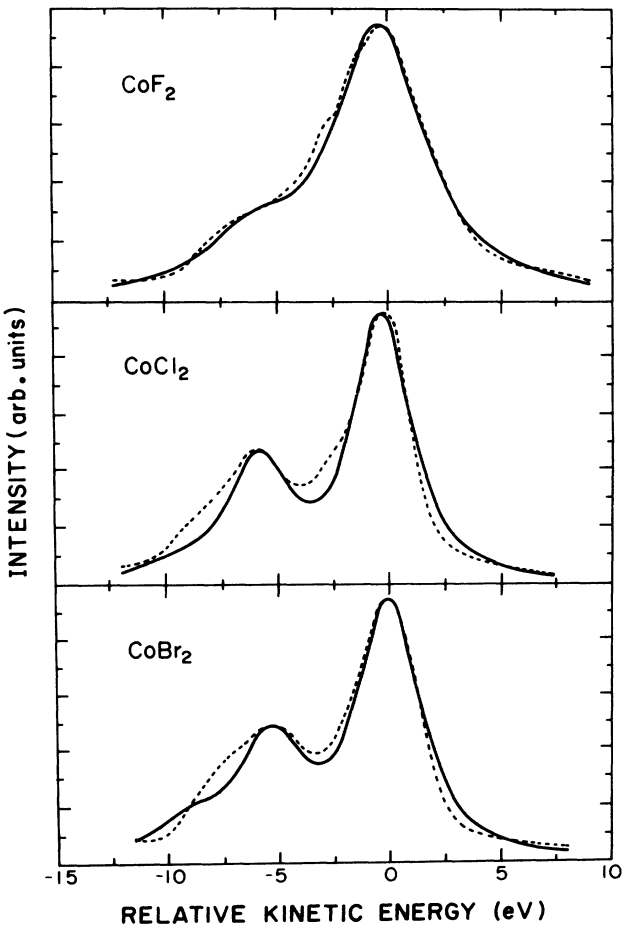

FIG. 4. Fits of the cluster model results with the experimental $2p_{3/2}$ spectra of the cobalt dihalides. The parameters used are listed in Table II. A Lorentzian broadening is 2.7, 3.2, and 4.4 eV for $CoCl_2$, $CpBr_2$, and CoF_2, respectively, and a Gaussian broadening of 1.2 eV (FWHM) was used.

TABLE I. Energy positions and intensities of satellites relative to the main peak obtained by decomposition of experimental spectra. ΔE denotes the binding-energy difference between the main and satellite peaks, and I_S and I_M denote the intensity of the satellite and main peaks, respectively.

Transition Metal	Compound	First satellite ΔE (eV)	First satellite I_S/I_M	Second satellite ΔE (eV)	Second satellite I_S/I_M
Co	CoF_2	5.8	0.18		
	$CoCl_2$	5.6	0.48	9.4	0.10
	$CoBr_2$	5.4	0.51	8.7	0.18
Fe	FeF_2	6.0	0.10		
	$FeCl_2$	5.4	0.42	8.6	0.03
	$FeBr_2$	5.2	0.48	8.3	0.12
Mn	MnF_2	6.4	0.06		
	$MnCl_2$	5.4	0.28		
	$MnBr_2$	5.2	0.38		

clearly, we include in this table the parameter values for copper and nickel dihalides determined in Refs. 2 and 24. The mixing matrix element T for bromides has been changed slightly to get better fits, but it is of minor importance.

We observe the following trends from this table. First for a given transition-metal element, the charge-transfer energy strongly depends on the ligand, and the values are in the order $\Delta_F > \Delta_{Cl} > \Delta_{Br}$ for all cations. This is as expected from the electronegativities of these halides. Secondly, the Coulomb energies Q and U ($U = 0.7Q$ was assumed throughout the series) increase as we go from

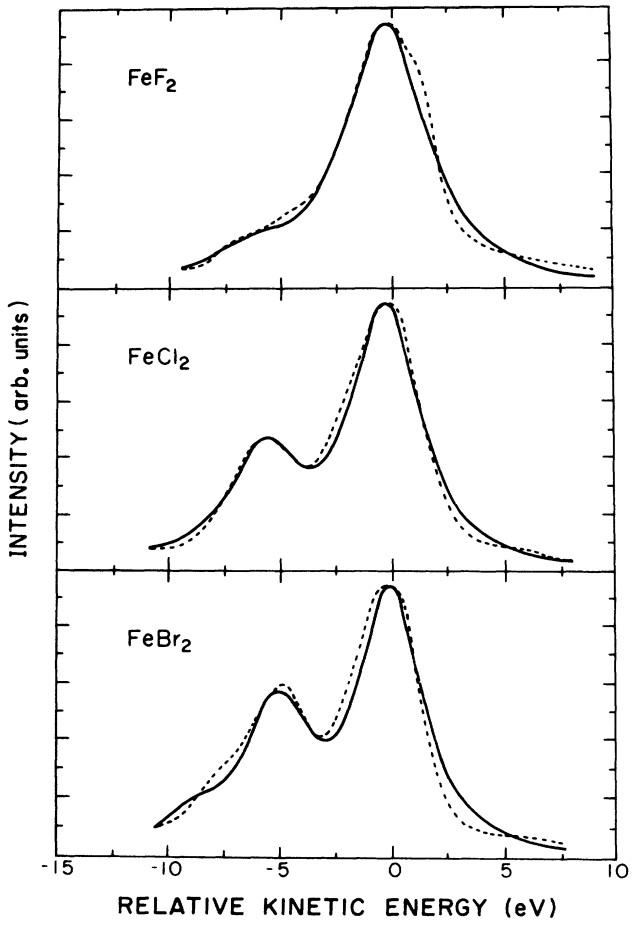

FIG. 5. Fits of the cluster model results with the experimental $2p_{3/2}$ spectra of the iron dihalides. The parameters used are listed in Table II. A Lorentzian broadening is 2.8, 3.2, and 4.0 eV for $FeCl_2$, $FeBr_2$, and FeF_2, respectively, and a Gaussian broadening of 1.2 eV (FWHM) was used.

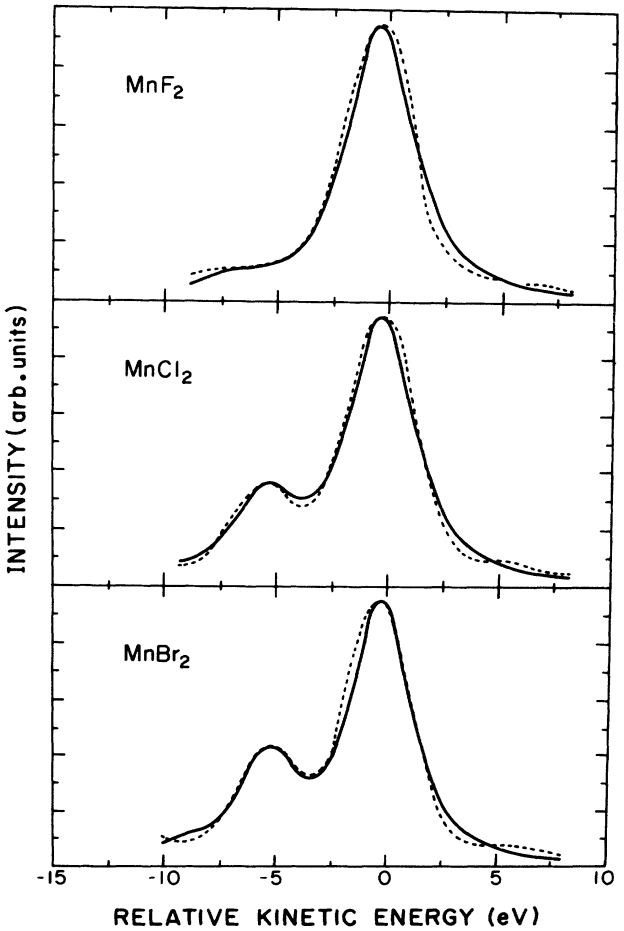

FIG. 6. Fits of the cluster model results with the experimental $2p_{3/2}$ spectra of the manganese dihalides. The parameters used are listed in Table II. A Lorentzian broadening is 2.6–3.0 eV, and a Gaussian broadening of 1.2 eV (FWHM) was used.

TABLE II. Parameter values and the ground-state 3d electron occupation number determined by the fit of transition-metal dihalides $2p_{3/2}$ core-level spectra. Δ, U, T, Q, and $\langle n_d \rangle$ denote the charge-transfer energy, d-d Coulomb interaction energy, metal d–ligand p mixing matrix element, core-hole–3d-electron Coulomb attraction energy, and the ground-state occupation number, respectively.

Transition metal	Compound	Δ (eV)	U (eV)	T (eV)	Q (eV)	$\langle n_d \rangle$
Cu	CuF_2	4.1	6.3	2.5	9.0	9.20
	$CuCl_2$	1.8	6.3	2.5	9.0	9.35
	$CuBr_2$	0.6	6.3	2.5	9.0	9.45
Ni	NiF_2	6.5	5.0	2.0	7.0	8.14
	$NiCl_2$	3.6	5.0	2.0	7.0	8.29
	$NiBr_2$	2.6	5.0	2.0	7.0	8.39
	NiI_2	1.5	4.5	2.0	7.0	8.53
Co	CoF_2	8.6	4.5	1.8	6.5	7.11
	$CoCl_2$	5.0	4.5	1.8	6.5	7.24
	$CoBr_2$	3.4	4.5	1.7	6.5	7.34
Fe	FeF_2	9.3	3.9	1.6	5.6	6.16
	$FeCl_2$	4.8	3.9	1.6	5.6	6.26
	$FeBr_2$	3.0	3.9	1.5	5.6	6.41
Mn	MnF_2	9.0	3.2	1.5	4.5	5.12
	$MnCl_2$	4.5	3.2	1.5	4.5	5.32
	$MnBr_2$	3.2	3.2	1.4	4.5	5.41

Mn to Cu. This is again expected due to the more localized 3d wave functions of the later transition metals, since Coulomb interaction tends to become larger for more localized levels. Thirdly, the ground-state 3d-level occupation number $\langle n_d \rangle$ increases from F to Br, as expected from the increased covalency of the latter compounds. The only trend that may be somewhat unexpected is the decrease of the T value as we go from Cu to Mn. Since the 3d wave function is more extended in earlier transition metals, T might be naively expected to increase, rather than decrease, as we go from Cu to Mn. However, lattice parameters also increase as we move from Cu to Mn, and these two effects tend to cancel each other. In fact, Mattheiss found from the band-structure calculation on transition-metal monoxides[31] that metal-oxygen overlap and covalency parameters are essentially constant for MnO, FeO, CoO, and NiO because of these canceling effects. The reason for the decrease, rather than being constant, of T values determined above is not clear at the moment, but it is probably due to many simplifications and neglected interactions of the model Hamiltonian.[23]

These parameter values should not be taken too literally. The parameter values of the model Hamiltonian may depend on which experiments it tries to describe. However, for a given experiment, they should be consistent as in Table II. Furthermore, these values are all within the expected range of parameters from various other spectroscopies.

V. THE EFFECT OF THE LIGAND BAND STRUCTURE AND THE CRYSTAL-FIELD SPLITTING

Although the cluster approximation was successful enough to give us confidence that the basic physics for the origin of satellite structures of these transition-metal dihalides is understood, there are some improvements that can be made in the model and the fit. For example, in fitting the data with the cluster model, we had to introduce a rather large Lorentzian broadening to mimic both the lifetime and multiplet effects. Also, the fit for the shape of the peaks, especially on bromide compounds, is less than perfect. To see if these can be improved by including effects omitted in our cluster model, we have investigated the effects of the ligand band dispersion and the crystal-field splitting $10Dq$.

The band effect of the ligand states is incorporated by dividing the continuous ligand band into discrete states and solving a huge matrix equation for the Green's function in the time domain as recently introduced by Gunnarsson and Schönhammer.[10] We follow the scheme used by Zaanen *et al.*[23] to calculate 2p core-level spectra of nickel dihalides by appropriately modifying matrix elements of the following Anderson-impurity Hamiltonian:

$$H_{\rm imp}+H_c=\sum_{\varepsilon,m,\sigma}[\varepsilon_{m\sigma}D(\varepsilon)+\Delta_{m\sigma}d^{\dagger}_{m\sigma}d_{m\sigma}] + \sum_{\substack{m\sigma\\ m',\sigma'}} U d^{\dagger}_{m\sigma}d_{m\sigma}d^{\dagger}_{m'\sigma'}d_{m'\sigma'} + \sum_{\varepsilon,m,\sigma}[V(\varepsilon)d^{\dagger}_{m\sigma}c_{\varepsilon m\sigma}+\text{H.c.}] + \sum_{m,\sigma}(n_c-1)Qd^{\dagger}_{m\sigma}d_{m\sigma}\ .$$

The 3d states in the cubic crystal field are split in energy by $10Dq$ into a triplet and a doublet state, but we neglect this difference in energy and treat them as degenerate here. The physical meaning of each parameter and its relevance to the cluster model should be obvious.

The basis states to be considered are restricted to the following three types only. One is the discrete state

$|d^n\rangle$, which has $n=5$, 6, and 7 for cations Mn^{2+}, Fe^{2+}, and Co^{2+}, respectively. Then we consider the continuum states $|d^{n+1}E\rangle$, describing a single charge-transfer state from the ligand level with energy E to the transition-metal $3d$ level. Finally, the double charge-transfer continuum states $|d^{n+2}EE'\rangle$ are considered. In principle, states with a higher number of the charge transfer should also be included. The cluster model calculation shows that these states significantly influence the energies and intensities of XPS final states through mixing effect, although they themselves do not gain much weight. However, inclusion of these states in our impurity calculation will make the matrices too large to be tractable, and we chose to neglect them. This causes some deviation of the parameter values (particularly T) determined by curve fitting in the impurity model from those of the cluster model where these higher charge-transfer states are also included as discrete states. Since we intend in this section only to demonstrate the influence of the band effect on the peak shapes, it will probably suffice to do with only these three sets of states. On the other hand, the parameter values should be compared with caution.

Denoting each of these sets of states as $|0\rangle$, $|E\rangle$, and $|EE'\rangle$, respectively, we get the following matrix elements of the Hamiltonian in the subspace:

$$\langle 0|H|0\rangle = 0 \quad \text{(reference)} ,$$

$$\langle E|H|E\rangle = \Delta - E ,$$

$$\langle EE'|H|EE'\rangle = 2\Delta + U - E - E' ,$$

$$\langle 0|H|E\rangle = (N_d)^{1/2} V(E) ,$$

$$\langle E|H|E'E''\rangle = \begin{cases} [2(N_d-1)]^{1/2} V(E) & \text{if } E=E'=E'' \\ [(N_d-1)]^{1/2} V(E'') & \\ & \text{if } E=E' \text{ and } E\neq E''. \end{cases}$$

Here N_d is 5, 4, and 3 for Mn^{2+}, Fe^{2+}, and Co^{2+}, respectively. All other matrix elements are zero. Since the ligand bands of these compounds are mostly 3–4 eV wide, we took the semielliptical band with a half bandwidth $B=1.87$ eV in this calculation. This band was divided into 21 discrete states yielding 253×253 coupled linear differential equation to solve. We followed the procedure in Refs. 10 and 23 to obtain the core-level spectral intensity. The optimal parameters of the curve fit, except for T, were found to be close to those determined in the cluster calculation of the previous section for all the compounds considered here. T values turned out to show systematic reduction of 10–20%, and this is a consequence of considering only states with charge transfer of up to two electrons.

An important observation from this impurity calculation result is the appearance of the asymmetric high-binding energy tails on each peak, which improves the fit in peak shapes for every compound. We do not rule out multiplet structures as the origin of these asymmetric peak shapes, but this calculation shows that the band

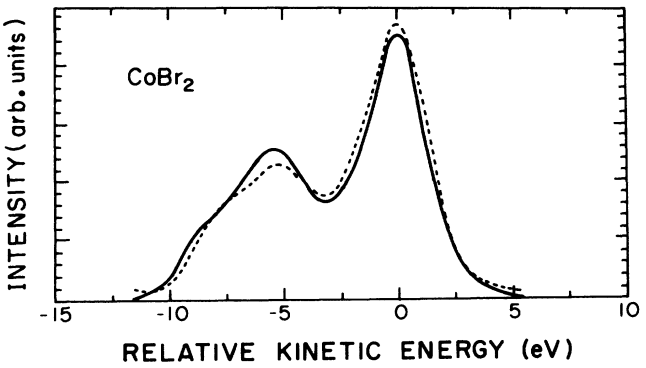

FIG. 7. A fit of the impurity-model result using $T=1.4$ eV, $\Delta=2.8$ eV, $Q=6.1$ eV, and $U=4.7$ eV with the experimental $2p_{3/2}$ spectra of the $CoBr_2$, where the band with a half width $B=1.87$ eV was divided into 21 discrete states. A Lorentzian lifetime broadening of 0.8 eV and a Gaussian broadening of 1.2 eV (FWHM) were used.

effect can also give a dominant contribution to the asymmetry of the peaks in these insulating compounds. The value of the Lorentzian broadening to mimic lifetime and multiplet effects is reduced by about a half compared with the result of the cluster model fit. Another thing to note is that the inclusion of the band effect seems to account for the uprise of the shoulder near the first satellite in $CoBr_2$. As shown in Fig. 7, the impurity model calculation gives an improved fit within the same parameter range. A similar situation has been encountered in the nickel dihalides $2p$ core-level XPS spectra.[23]

Let us now briefly mention the effect of the $3d$-level crystal-field splitting $10Dq$. In our cluster model calculations in Sec. III, we took into account the crystal-field-splitting energy $10Dq$ when determining the ground-state symmetry of transition-metal dihalides, while we neglected it when setting up the XPS model Hamiltonian. For consistency, we should have included $10Dq$ when calculating XPS intensity as well. In the case of Co^{2+}, for example, this results in the 6×6 Hamiltonian matrix to diagonalize instead of 4×4, and then two new satellites will appear. We have actually performed the calculation with the parameter $10Dq/T=0.5$ for Co^{2+} as a test case. [For the compounds discussed here, $10Dq$ values are about 1 eV (Ref. 32)]. We found that new satellites appear at the positions between the main and the first satellite peaks, and between the first and the second satellites. However, the relative intensities of these new satellites are very small (less than 0.02) in the parameter ranges of our interest. Also, other satellite peaks do not show much change in position and intensity. This seems to indicate that the crystal-field-splitting energy $10Dq$ does not play a significant role in determining the $2p$ core-level XPS spectra of these transition-metal dihalide compounds.

VI. CONCLUSION AND OUTLOOK

Many models have been proposed so far for the origin of the satellite structure in the $2p$ core-level XPS spectra of $3d$ transition-metal compounds. Among these, the

charge-transfer model of Larsson[19] and Sawatzky *et al.*,[21–23] which takes into account the core-hole–3*d*-electron Coulomb attraction in the final state, seems to be the most suitable at least for heavy-transition-metal dihalides. Unlike other models, which are concerned mostly only with the energy separations of satellites, this charge-transfer model accounts for the *energy separations and intensities* of satellites quantitatively. The values of the parameters of the model Hamiltonian are in reasonable ranges and show consistent trends. Applying this model we can get information on the valence-electronic structures of the correlated electron systems by studying their core-level satellites. Another piece of physics we learned from the success of this model is that the screening response is important in the presence of a core hole even for insulators. The importance of screening has been generally realized for metallic systems, but not so widely accepted for insulators as yet.

The question naturally arises whether this charge-transfer model can explain satellite structures of *all* the transition-metal core-level spectra. The answer unfortunately seems to be a negative when we surveyed experimental data from the published literature. For example, $CrCl_3$ and $CrBr_3$ 2*p* XPS show satellites located at ~ 15 eV away from the main line,[28] which is too big an energy separation to be explained by the charge-transfer model with reasonable parameters. Even for compounds with an Fe cation, $K_4Fe(CN)_6$ shows a 2*p* satellite at ~ 14 eV from the main line,[5] again too far away to be a reasonable charge-transfer satellite. Therefore, depending on the ligands or cations, there seems to be different mechanisms that give rise to satellite structures. In this connection it may be worthwhile to mention the exciton satellite mechanism,[33] which dominates over the charge-transfer satellites when Δ is large, Q is small, and there are many empty 3*d* orbitals. Therefore, exciton satellites should be prominent in early transition-metal compounds, which seems to be consistent with experimental data.

ACKNOWLEDGMENTS

One of the authors (S.J.O.) thanks Professor G. A. Sawatzky, Dr. A. Fujimori, and Professor A. Kotani for useful discussions. This work was supported in part by Korea Science and Engineering Foundation (KOSEF).

*Author to whom all correspondence should be addressed.

[1]See, for a review, G. Wendin, Struct. Bonding (Berlin) **45**, 1 (1981).

[2]G. K. Wertheim, R. L. Cohen, A. Rosencwaig, and H. J. Guggenheim, in *Electron Spectroscopy,* edited by D. A. Shirley (North-Holland, Amsterdam, 1972), p. 813.

[3]A. J. Signorelli and R. G. Hayes, Phys. Rev. B **8**, 81 (1973).

[4]C. K. Jorgensen and H. Berthou, Chem. Phys. Lett. **13**, 186 (1972).

[5]T. A. Carlson, J. C. Carver, and G. A. Vernon, J. Chem. Phys. **62**, 932 (1975).

[6]G. A. Vernon, G. Stucky, and T. A. Carlson, Inorg. Chem. **15**, 278 (1976).

[7]D. C. Frost, C. A. McDowell, and I. S. Woolsey, Chem. Phys. Lett. **17**, 320 (1972).

[8]A. Kotani and Y. Toyozawa, J. Phys. Soc. Jpn. **35**, 1073 (1973); **35**, 1082 (1973); **37**, 912 (1974).

[9]S.-J. Oh and S. Doniach, Phys. Rev. B **26**, 2085 (1982).

[10]O. Gunnarsson and K. Schönhammer, Phys. Rev. B **28**, 4315 (1983); **31**, 4815 (1985).

[11]J. C. Fuggle, M. Campagna, Z. Zolnierek, R. Lässer, and A. Platau, Phys. Rev. Lett. **45**, 1597 (1980).

[12]J. C. Fuggle, F. U. Hillebrecht, Z. Zolnierek, R. Lässer, Ch. Freiburg, O. Gunnarsson, and K. Schönhammer, Phys. Rev. B **27**, 7330 (1983).

[13]W.-D. Schneider, B. Delley, E. Wuilloud, J.-M. Imer, and Y. Baer, Phys. Rev. B **32**, 6819 (1985).

[14]R. P. Gupta and S. K. Sen, Phys. Rev. B **12**, 15 (1975).

[15]A. Rosencwaig, G. K. Wertheim, and H. J. Guggenheim, Phys. Rev. Lett. **27**, 479 (1971).

[16]K. S. Kim, J. Electron Spectrosc. Relat. Phenom. **3**, 217 (1974).

[17]D. A. Shirley, Chem. Phys. Lett. **16**, 220 (1972); L. Ley, S. P. Kowalczyk, F. R. McFeely, R. A. Pollak, and D. A. Shirley, Phys. Rev. B **8**, 2392 (1972).

[18]B. Johansson and N. Mårtensson, Phys. Rev. B **21**, 4427 (1980); **24**, 4484 (1981).

[19]S. Larsson, Chem. Phys. Lett. **32**, 401 (1975); **40**, 362 (1976); S. Larsson and M. Braga, *ibid.* **48**, 596 (1977).

[20]B. W. Veal and A. P. Paulikas, Phys. Rev. B **31**, 5399 (1985).

[21]G. van der Laan, C. Westra, C. Haas, and G. A. Sawatzky, Phys. Rev. B **23**, 4369 (1981).

[22]G. A. Sawatzky, in *Studies in Inorganic Chemistry,* edited by R. Metselaar, H. J. M. Heijligers, and J. Schoonman (Elsevier, Amsterdam, 1983), Vol. 3, p. 3.

[23]J. Zaanen, C. Westra, and G. A. Sawatzky, Phys. Rev. B **33**, 8060 (1986).

[24]S. Sugano, Y. Tanabe, and H. Kamimura, *Multiplets of Transition-Metal Ions in Crystals* (Academic, New York, 1970).

[25]G. W. Pratt, Jr. and R. Coelho, Phys. Rev. **116**, 281 (1959).

[26]S. P. Kowalczyk, F. R. McFeely, L. Ley, and D. A. Shirley, in *Magnetism and Magnetic Materials,* edited by C. D. Graham *et al.* (AIP, New York, 1975), p. 207.

[27]J. Zaanen and G. A. Sawatzky, Phys. Rev. B **33**, 8074 (1986).

[28]M. Okusawa, Phys. Status Solidi B **124**, 673 (1984).

[29]E. Antonides, E. C. Janse, and G. A. Sawatzky, Phys. Rev. B **30**, 1669 (1977).

[30]G. A. Sawatzky and F. van der Woude, J. Phys. (Paris) Colloq. **35**, C6-47 (1974).

[31]L. F. Mattheiss, Phys. Rev. B **5**, 290 (1972); **5**, 306 (1972).

[32]E. Sacher, Phys. Rev. B **34**, 5130 (1986).

[33]D. K. G. de Boer, C. Haas, and G. A. Sawatzky, Phys. Rev. B **29**, 4401 (1984).